Spectrosc. Lett. 13 (1980)
R.M. Leblanc, Rev. Sci.
and R.M. Leblanc, Pho-
ii. B. Szych and R.M.
(1986) 121.
. Eur. J. Biochem. 143
of aromatic molecules
'0).
nic and Z. Gryczynski,

Journal of Luminescence 39 (1987) 11–17
North-Holland, Amsterdam

THE INFLUENCE OF THE CONCENTRATION OF Er^{3+} IONS ON THE CHARACTERISTICS OF AC-ELECTROLUMINESCENCE IN ZnS : ErF_3 THIN FILMS

Li-Jian MENG, Chang-hua LI and Guo-zhu ZHONG

Changchun Institute of Physics, Academia Sinica, Changchun, People's Rep. China

Received 9 April 1987
Accepted 25 June 1987

We have investigated the influence of the concentration of Er ions on the characteristics of ACEL (AC-electroluminescence) in ZnS : ErF_3 thin films. It is found that $I(^4F_{9/2}-{}^4I_{15/2})$ depends strongly on the concentration of Er ions. $I(^4F_{9/2}-{}^4I_{15/2})$ increases with the concentration and even exceeds $I(^2H_{11/2}-{}^4I_{15/2})$ at higher concentration. By studying the EL (electroluminescence) decay, the variation of the ratio of green to red with applied voltage and EL efficiency of emissions from $^2H_{11/2}+{}^4S_{3/2}$ to $^4I_{15/2}$ and from $^4F_{9/2}$ to $^4I_{15/2}$ for samples with a different concentration of Er ions, we consider that the increase of $I(^4F_{9/2}-{}^4I_{15/2})$ is mainly due to the cross-relaxation process. It is also found that the interaction between Er ions is attributed to the interaction between two dipoles.

1. Introduction

The recent growth of interest in an AC ZnS : Mn thin film EL has been brought about by the remarkable sucess of the development of EL display panels with high brightness, long life and good stability. Since the emission color of the ZnS : Mn EL panels is limited only to yellowish-orange, enormous efforts have been carried out to develop multicolor thin film EL devices. The ZnS thin film ACEL devices doped with trivalent rare earth ions have attractive prospects for the color EL display panels. Many studies on the luminescence characteristics of trivalent rare-earth ions doped ZnS thin-film devices have been reported [1–10], but studies of excitation mechanisms and luminescence centers predominate. A few attempts have been made to study interaction between ions [4,6]. Recently, Kobayashi et al. [6] have reported the ACEL characteristics of ZnS thin films doped with TbF_3, SmF_3 and TmF_3. They have studied the interaction between ions and given a model of cross-relaxation. So far, no detailed study on the influence of concentration of Er ions on the characteristics of ACEL in ZnS : ErF_3 thin films have been reported. By studying the influence of the concentration of Er ions on brightness, efficiency and EL decay in ZnS : ErF_3 thin films, we can obtain the optimum value of Er ions concentration in ZnS : ErF_3 thin films, and understand the EL basic process and concentration quenching mechanism. It is significant to improve the performance of ZnS : ErF_3 thin film devices.

In this study, we have fabricated ZnS : ErF_3 thin film samples with various Er concentration by electron beam evaporation. By measuring and analyzing the EL characteristics of the samples, we first propose the cross-relaxation process occurring between Er ions and explain experimental phenomena.

2. Device fabrication

Thin-film ZnS EL devices with various Er concentrations 0.03, 0.3, 1, 5 and 30 wt% have been prepared. The EL device structures are shown in fig. 1. The devices have the conventional structure of doubly insulating layers, ITO–Y_2O_3–ZnS : ErF_3–Y_2O_3–Al. The devices are prepared by sequential depositions of Y_2O_3 insulating layer, ZnS : ErF_3 EL emission layer, Y_2O_3 again and Al

0022-2313/87/$03.50 © Elsevier Science Publishers B.V.
(North-Holland Physics Publishing Division)

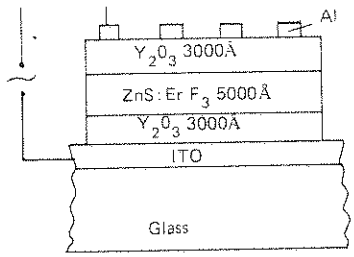

Fig. 1. Structure of sample used in the studies.

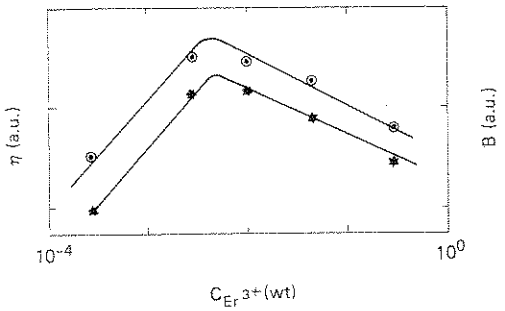

Fig. 2. Activator concentration dependences of the brightness B (⊙) and EL efficiency η (*) (1 kHz sine wave).

electrode onto an indium–tin–oxide (ITO)-coated glass plate. The depositions of Y_2O_3 and ZnS : ErF_3 layers are carried out by electron-beam evaporation. The thickness of Y_2O_3 and the ZnS : ErF_3 layer are 3000 Å and 5000 Å, respectively. Before evaporation, the ZnS powder is fired in S atmosphere for about 1 h at around 1050 °C, then the ErF_3 is mixed with the ZnS powder, the mixture is ground mechanically and then pressed into slices under about 100 atm.

3. Experimental results

Samples A, B, C, D and E denote that the concentration of Er ions are 0.03, 0.3, 1, 5 and 30 wt%, respectively.

Figure 2 shows the dependences of the saturation brightness B and maximum EL emission efficiency η on the Er concentration in EL devices. The result indicates that an optimum concentration is about 1 wt%. The increase in brightness and efficiency with concentration at low doping levels results simply from an increased number of luminescence centres. As the doping level is further increased, the periodicity of the crystalline field is destroyed. The hot electrons lose their energy by collisions and the energy function of hot electrons shifts toward the low energy direction. Concentration quenching may also play a part at these doping levels.

We have measured the ACEL spectra of these samples at room temperature and 77 K. The range of measurement is from 350 to 700 nm which includes seven groups of spectral lines. The spectral line positions and corresponding transitions are listed in table 1. The energy levels of Er ions are shown in fig. 3(c). Figure 3(a) shows the ACEL spectra of samples A, C and E at room temperature. Figure 3(b) shows the ACEL spectra of sample E at room temperature and liquid nitrogen temperature. We have found that $I(^4F_{9/2}-{}^4I_{15/2})$ increases obviously with the concentration of Er ions and temperature. As the Er concentration increases, the periodicity of the crystalline field is entirely destroyed. The mean free path of hot electrons is shortened. The results will enhance the emission of low lying levels of Er ions. However, the hot electron energy distribution will still shift to higher energies by increasing the voltage across the sample. Namely, the ratio of green to red should increase with applied voltage [8]. We have measured the dependence of the $I(^2H_{11/2}+{}^4S_{3/2}-{}^4I_{15/2})/I(^4F_{9/2}-{}^4I_{15/2})$ on applied voltage, as shown in fig. 4. It is shown that the ratio of green to red increases with applied voltage when the Er concentration is 0.03 wt%,

Table 1
Spectra position of the lines in the EL spectrum of ZnS : ErF_3 thin film

	Transition	Wavelength (nm)	Wavenumber (cm^{-1})
I_1	$^4G_{11/2}-{}^4I_{15/2}$	384	26040
I_2	$^2H_{9/2}-{}^4I_{15/2}$	410	24390
I_3	$^4F_{3/2}+{}^4F_{5/2}-{}^4I_{15/2}$	458	21830
I_4	$^4F_{7/2}-{}^4I_{15/2}$	494	20240
I_5	$^2H_{11/2}-{}^4I_{15/2}$	525	19030
I_6	$^4S_{3/2}-{}^4I_{15/2}$	547	18280
I_7	$^4F_{9/2}-{}^4I_{15/2}$	660	15160
		673	14870

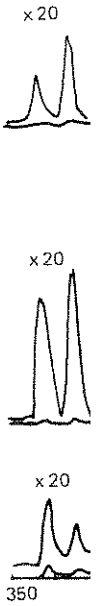

Fig. 3. (a) ACEL s

while it decrea
age when the
0.3%. The res
increase of $I($
decrease of th
Figure 5 sh
and $^4F_{9/2}$ leve

Table 2
Data of EL deca

C (wt)	^2H
	J_1
3×10^{-3}	1
1×10^{-2}	1
5×10^{-2}	1
3×10^{-1}	1

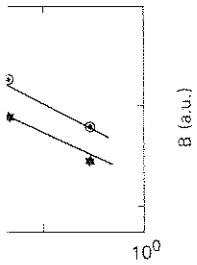

dences of the brightness
1 kHz sine wave).

ıre 3(a) shows the
C and E at room
s the ACEL spectra
erature and liquid
have found that
ously with the con-
perature. As the Er
periodicity of the
:stroyed. The mean
ortened. The results
)w lying levels of Er
on energy distribu-
ergies by increasing
Namely, the ratio of
vith applied voltage
dependence of the
$^2H_{9/2}$–$^4I_{15/2}$) on ap-
4. It is shown that
reases with applied
ration is 0.03 wt%,

L spectrum of ZnS : ErF_3

ngth	Wavenumber (cm^{-1})
	26040
	24390
	21830
	20240
	19030
	18280
	15160
	14870

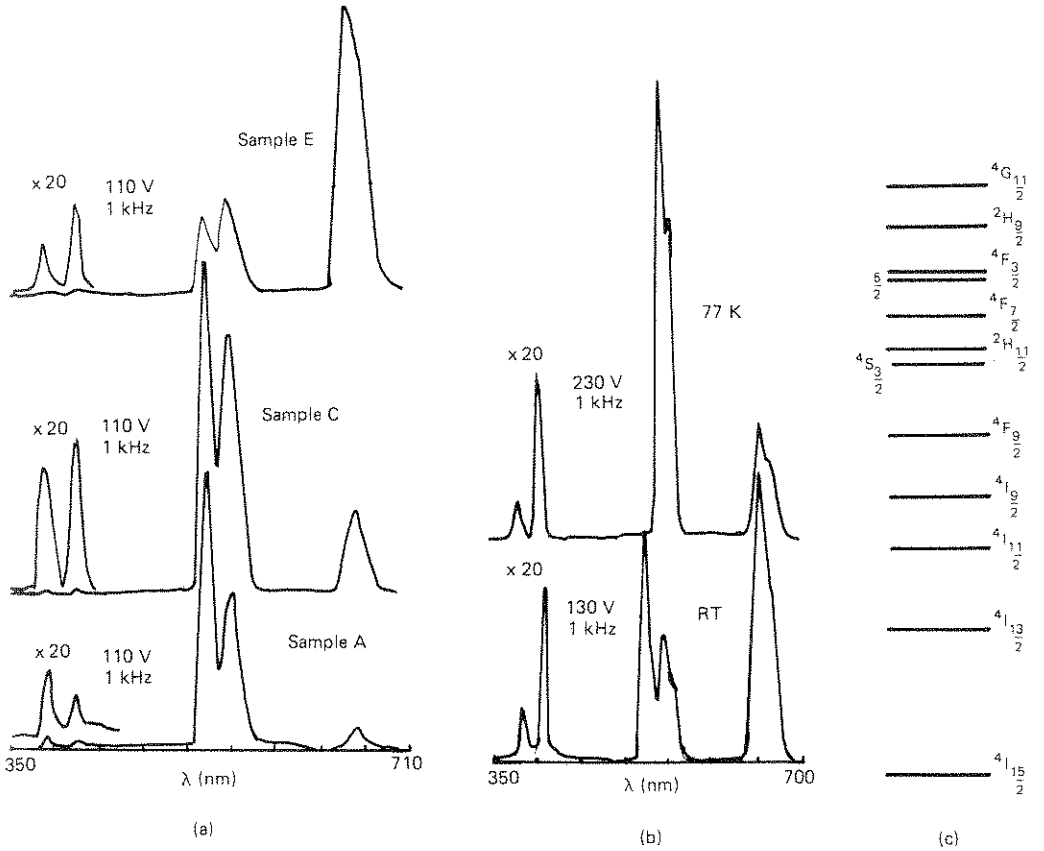

Fig. 3. (a) ACEL spectra of samples A (0.03 wt%), C (1.0 wt%) and E (30 wt%) at RT (corrected); (b) ACEL spectra of sample E at RT and 77 K (uncorrected); (c) Energy levels of Er^{3+}.

while it decreases with increasing the applied voltage when the Er ion concentration is more than 0.3%. The results suggest that the reason for the increase of $I(^4F_{9/2}-^4I_{15/2})$ is not only due to the decrease of the mean free path of the hot electron.

Figure 5 shows the EL decay of $^2H_{11/2}$, $^4S_{3/2}$ and $^4F_{9/2}$ levels in sample E. It is found that the EL decay of $^2H_{11/2}$ and $^4S_{1/2}$ levels may be divided into two exponential components of fast and slow decay. We can fit the decay curves of $^2H_{11/2}$ and $^4S_{3/2}$ levels to the formula $J = J_{10}\exp(-t/\tau_1) + J_{20}\exp(-t/\tau_2)$, where J_{10} and J_{20} are the luminescence intensities of slow and fast components at $t = 0$, respectively. τ_1 and τ_2

Table 2
Data of EL decay of samples with different Er^{3+} concentration

C (wt)	$^2H_{11/2}$					$^4S_{3/2}$					$^4F_{9/2}$
	J_{10}	τ_1 (μs)	J_{20}	τ_2 (μs)	$\frac{J_{20}}{J_{10}}$	J_{10}	τ_1 (μs)	J_{20}	τ_2 (μs)	$\frac{J_{20}}{J_{10}}$	τ (μs)
3×10^{-3}	135	60	25	25	0.20	110	60	30	25	0.27	75
1×10^{-2}	110	60	48	20	0.36	72	60	38	20	0.59	85
5×10^{-2}	140	60	60	18	0.45	80	60	55	18	0.69	120
3×10^{-1}	100	55	130	13	1.30	72	55	128	13	1.78	180

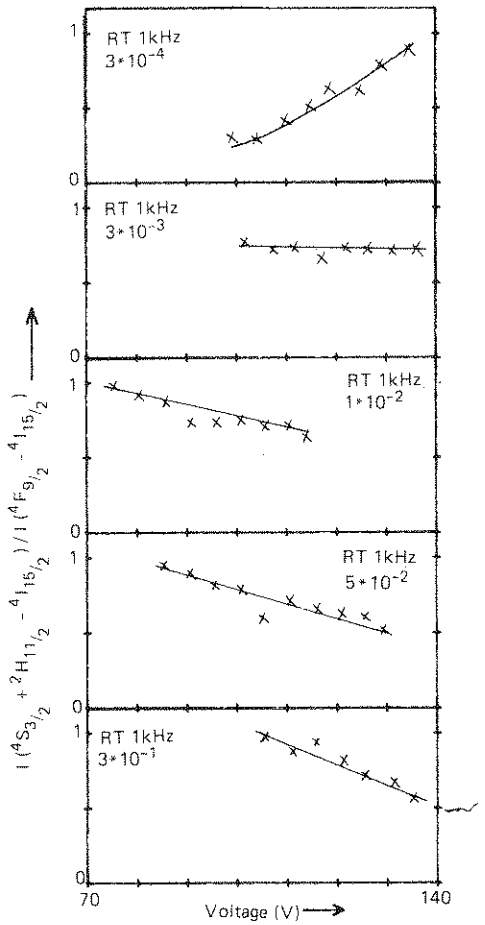

Fig. 4. Voltage dependences of intensity ratio of samples with different Er^{3+} ion concentration.

are the decay times of slow and fast components, respectively. EL decay of the $^4F_{9/2}$ level is approximately fitted to the formula $J = J_0 \exp(-t/\tau)$. The data of EL decay are listed in table 2. It should be noted from table 2, that there are some important results. With increasing Er concentration the EL decay time of the $^4F_{9/2}$ level increases from 75 μs at 0.03% to 180 μs at 30%. The EL decay time of the slow component of $^2H_{11/2}$ and $^4S_{3/2}$ levels nearly remains constant. But the EL decay time of the fast component of $^2H_{11/2}$ and $^4S_{3/2}$ levels decreases and becomes the predominant component in EL decay with increasing Er ion concentration.

We have also measured the dependence of EL

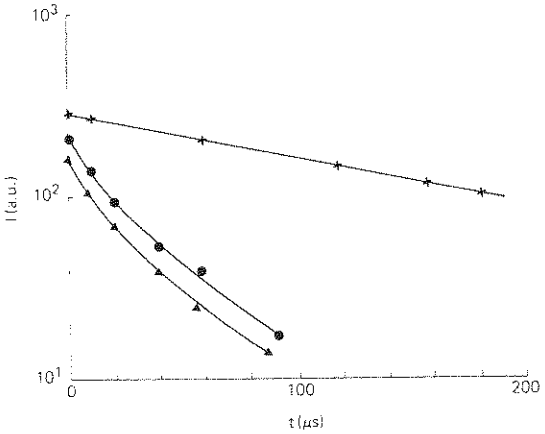

Fig. 5. EL decay curve of $^2H_{11/2}$ (●), $^4S_{3/2}$ (▲) and $^4F_{9/2}$ (×) emission of sample E (30 wt%) at room temperature.

efficiency of emissions from $^2H_{11/2} + {}^4S_{3/2}$ to $^4I_{15/2}$ and from $^4F_{9/2}$ to $^4I_{15/2}$ on the concentration of Er ions in ZnS thin films, as shown in fig.

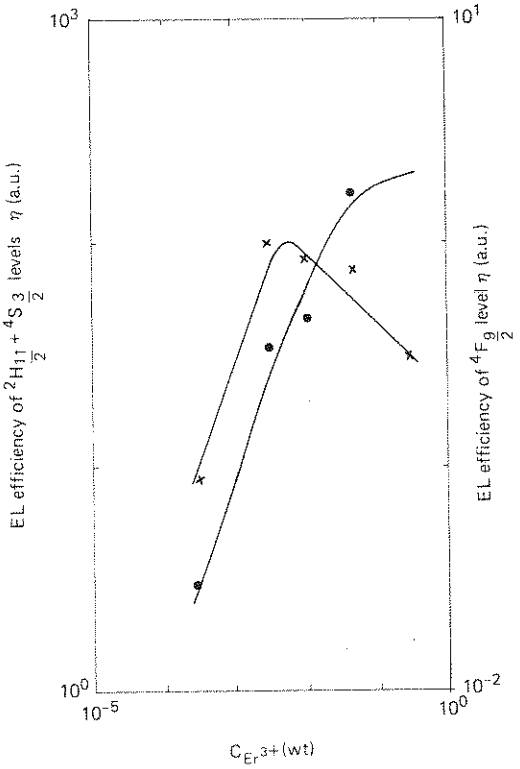

Fig. 6. Activator concentration dependences of EL efficiency of $^2H_{11/2} + {}^4S_{3/2}$ levels (×) and $^4F_{9/2}$ level (●) (1 kHz sine wave).

6. It is shown
from $^2H_{11/2} + {}^4$
concentration,
and then falls
increases with
saturates at 5%
that the conce
level are differ
centration quer
is usually ment

4. Discussion

The experim
gest that with
the interaction
ously and resu
$^4S_{3/2}$ excited
populations lo
their energies
creases with th
EL efficiency
continuously i
obvious that t
stronger the e
Therefore, it is
the concentrat
tween Er ions
radiative relax
$^4S_{3/2}$ excited
results lead to
$^2H_{11/2}$ and ^{4}
emission from

From the d
(table 2) it is s
decay of $^2H_{11}$
predominant
are two kinds
by the intera
decays corres
respectively. V
of Er ions, the
increases, the
predominant.
EL decay tim
with Er conc
result is mai
tions of $^2H_{11}$

6. It is shown that the EL efficiency of emission from $^2H_{11/2}+{}^4S_{3/2}$ to $^4I_{15/2}$ increases with Er ion concentration, reaches a maximum value at 0.03% and then falls down; but that from $^4F_{9/2}$ to $^4I_{15/2}$ increases with Er ion concentration and finally saturates at 5%. For the first time, we observed that the concentration quenching values of each level are different for Er ions. Therefore, the concentration quenching value of rare earth ions which is usually mentioned is not exact.

4. Discussion

The experimental results mentioned above suggest that with increasing concentration of Er ions, the interaction between Er ions increases obviously and results in the quenching of $^2H_{11/2}$ and $^4S_{3/2}$ excited states (fig. 6); namely, part of the populations located in these excited states will lose their energies nonradiatively and this quantity increases with the concentration of Er ions. But the EL efficiency of emission from $^4F_{9/2}$ to $^4I_{15/2}$ continuously increases (fig. 6). From fig. 3, it is obvious that the higher the Er concentration, the stronger the emission intensity of $^4F_{9/2}$ to $^4I_{15/2}$. Therefore, it is concluded that with an increase of the concentration of Er ions, the interaction between Er ions also increases and results in nonradiative relaxation of Er ions from $^2H_{11/2}$ and $^4S_{3/2}$ excited states to $^4F_{9/2}$ excited state. These results lead to the quenching of emission from $^2H_{11/2}$ and $^4S_{3/2}$ to $^4I_{15/2}$ and the increase of emission from $^4F_{9/2}$ to $^4I_{15/2}$.

From the data of the EL decay of the samples (table 2) it is shown that the fast component of EL decay of $^2H_{11/2}$ and $^4S_{3/2}$ excited states becomes predominant and the decay time decreases. There are two kinds of centers which are distinguished by the interaction between Er ions. Their EL decays correspond to fast and slow components, respectively. With an increase of the concentration of Er ions, the number of centres with interaction increases, therefore, the fast component becomes predominant. From table 2 we have found that the EL decay time of the $^4F_{9/2}$ excited state increases with Er concentration. It is supposed that this result is mainly due to the nonradiative relaxations of $^2H_{11/2}$–$^4F_{9/2}$ and $^4S_{3/2}$–$^4F_{9/2}$.

Nonradiative relaxation between electronic states of Er ions occurs usually by multi-phonon emission or by cross relaxation [6]. The former has been excepted [11]. The latter involves the interaction between an excited activator ion and one (or more) neighboring ground state ions which have approximately the same energy gap as the energy gap across which the relaxation is to occur. However, according to the energy levels of Er ions, the energy gaps of $^2H_{11/2}$–$^4F_{9/2}$ and $^4S_{3/2}$–$^4F_{9/2}$ are less than that of $^4I_{15/2}$–$^4I_{13/2}$. Therefore, the cross-relaxation will only occur between excited Er ions. When the concentration of Er ions exceeds 0.03%, the decrease of the ratio of green to red with an increase of applied voltage, as shown in fig. 4, suggests that the increase of the applied voltage, i.e. the increase of exciting density, is favourable for the cross-relaxation process. This result provides important proof for the cross-relaxation process between excited Er ions.

To find concrete cross-relaxation processes, we have measured the ratio of EL emission intensity of all excited states (within the range of measurement) to that of the $^4G_{11/2}$ excited state, as shown in fig. 7. It is shown that the ratios decrease except $I(^2H_{9/2})/I(^4G_{11/2})$ and $I(^4F_{9/2})/I(^4G_{11/2})$ with an increase of the concentration of Er ions. Therefore, it is concluded that EL emission of $^2H_{9/2}$ and $^4F_{9/2}$ excited states increases and that of $^4F_{7/2}$, $^4F_{5/2}+{}^4F_{3/2}$ and $^2H_{11/2}+{}^4S_{3/2}$ excited states decreases with increasing the concentration of Er ions. According to the results, we may suppose the concrete cross-relaxation process, as shown in fig. 8. The energy mismatch will be compensated by phonons. The influence of temperature (Fig. 3(b)) implies that the phonons will take part in the cross-relaxation process.

With increasing the concentration of Er ions in ZnS thin films, the interaction between Er ions will also increase and the nonradiative energy transfer processes will occur between Er ions. The energy transfer probability is usually written in the form [12]

$$p=\frac{3e^4}{8\pi^2 m^2 C^3 n^4 R^5 \bar{\nu}^2}\times\sum_{if'}\left[f_{if}^{s}f_{i'f'}^{a}\int F_{if}^{s}(\bar{\nu})F_{i'f'}^{a}(\bar{\nu})\,\mathrm{d}\bar{\nu}\right]=C\cdot R^{-s},$$

200

$^4S_{3/2}$ (▲) and $^4F_{9/2}$ (×) at room temperature.

n $^2H_{11/2}+{}^4S_{3/2}$ to $_{/2}$ on the concentralms, as shown in fig.

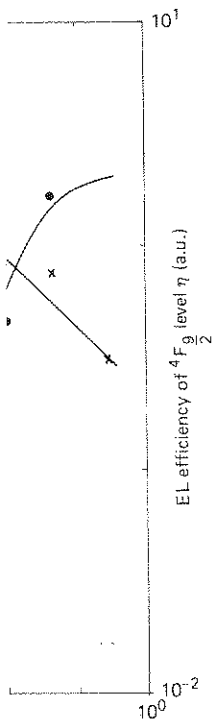

endences of EL efficiency $F_{9/2}$ level (●) (1 kHz sine

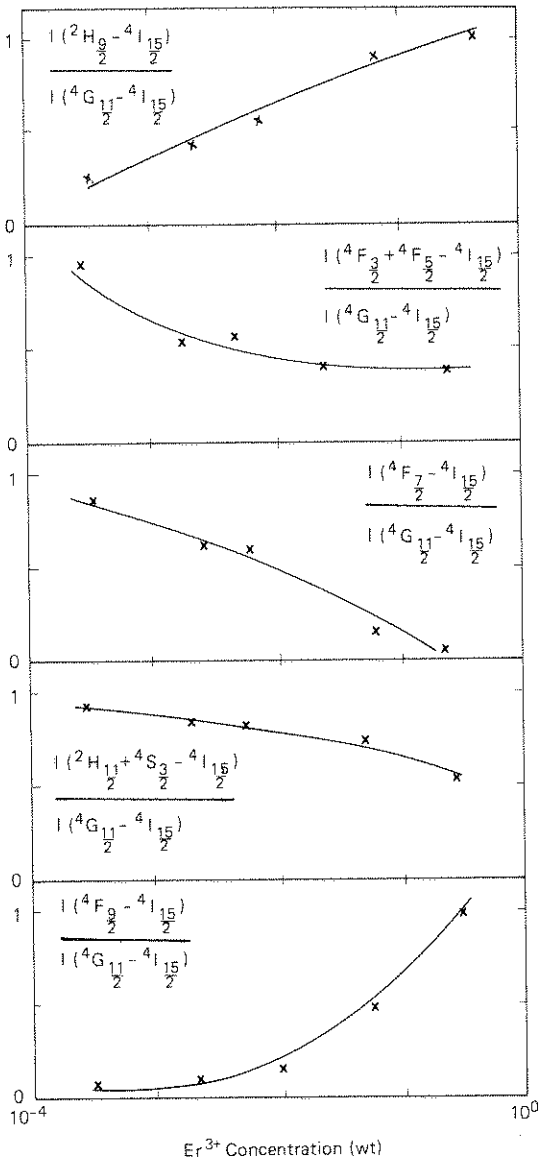

Fig. 7. Activator concentration dependences of intensity ratio of EL spectrum (1 kHz, 110 V sine wave RT).

Table 3
Cross-relaxation rate of samples with different Er concentration

$C_{Er^{3+}}$ (wt)	3×10^{-3}	1×10^{-2}	5×10^{-2}	3×10^{-1}
$f(s^{-1})$	2.3×10^4	3.3×10^4	3.9×10^4	5.9×10^4

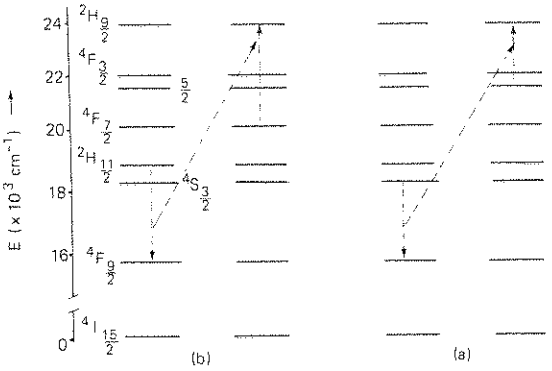

Fig. 8. Possible cross-relaxation processes.

where C is the energy transfer constant, f_{if}^{s} and $f_{i'f'}^{a}$ are the oscillator strengths, F_{if}^{s} and $F_{i'f'}^{a}$ are the line-shape functions, n is the index of refraction, R is the distance between the ions and the value of s can be 6, 8 and 10, depending on whether the interaction involved is dipole–dipole, dipole–quadrupole, or quadrupole–quadrupole.

The nonradiative transition probability of $^2H_{11/2}$ and $^4S_{3/2}$ excited states is given [13] by $f = 1/\tau_2 - 1/\tau_1$, where τ_2 and τ_1 are the EL decay time of fast and slow components, respectively. We calculated the relaxation rate f by using the data in table 2. The results are listed in table 3. It is found that f is proportional to the second power of the concentration of Er ions (fig. 9), namely, inversely proportional to the sixth power of distance R between two ions. Therefore, the interaction is attributed to the interaction between two dipoles [12].

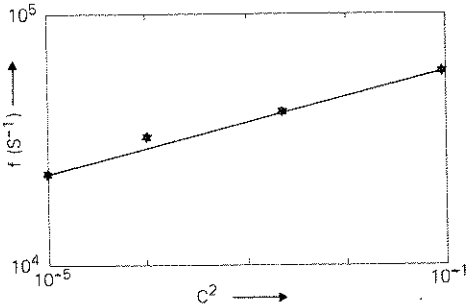

Fig. 9. f vs C^2 at room temperature.

5. Conclusion

(1) For th
$I(^4F_{9/2}-{}^4I_{15/}$
ceeds $I(^2H_{11}$
Er ions is ove
(2) We f
quenching va
in ZnS : ErF_3
(3) By stu
with differen
that the incre
to the cross-r
decays nonra
the $^4F_{9/2}$ stat
from $^4F_{5/2}$ o
(4) By cal
is indicated
belongs to di

Acknowledge

The autho
Mrs. Guan

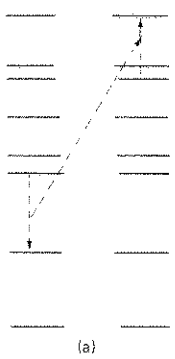

(a)

on processes.

er constant, f_{if}^{s} and
is, F_{if}^{s} and $F_{i'f'}^{a}$ are
the index of refrac-
en the ions and the
l 10, depending on
ed is dipole–dipole,
pole–quadrupole.
ion probability of
tes is given [13] by
τ_1 are the EL decay
onents, respectively.
rate f by using the
e listed in table 3. It
onal to the second
of Er ions (fig. 9),
l to the sixth power
ions. Therefore, the
interaction between

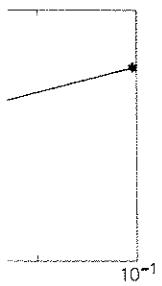

mperature.

5. Conclusions

(1) For the first time, it is observed that $I(^4F_{9/2}-{}^4I_{15/2})$ increases obviously and even exceeds $I(^2H_{11/2}-{}^4I_{15/2})$ when the concentration of Er ions is over 0.3 wt%.

(2) We first find that the concentration quenching value of each excited state is different in ZnS : ErF_3 thin films.

(3) By studying EL characteristics of samples with different Er ion concentration, we proposed that the increase of $I(^4F_{9/2}-{}^4I_{15/2})$ is mainly due to the cross-relaxation process in which one Er ion decays nonradiatively from the $^2H_{11/2}$ or $^4S_{3/2}$ to the $^4F_{9/2}$ state while exciting a neighboring Er ion from $^4F_{5/2}$ or $^4F_{7/2}$ state to $^2H_{9/2}$ state.

(4) By calculating the cross-relaxation rate f, it is indicated that the interaction between Er ions belongs to dipole–dipole interaction.

Acknowledgements

The authors wish to thank Mr. Yu Bao-gui and Mrs. Guan Zhong-su for their help in the experiments, Mr. Zhao Guo-zhang for his help with the preparation of the samples.

References

[1] D. Kahng, Appl. Phys. Lett. 13 (1968) 210.
[2] E.W. Chase et al., J. Appl. Phys. 40 (1969) 2512.
[3] H. Kobayashi et al., J. Appl. Phys. 13 (1974) 1110.
[4] J. Benoit et al., J. Lumin. 23 (1981) 175.
[5] D.C. Krupka et al., J. Appl. Phys. 43 (1972) 2314.
[6] H. Kobayashi et al., Phys. Stat. Sol(a) 88 (1985) 713.
[7] D.C. Krupka et al., J. Appl. Phys. 43 (1972) 476.
[8] H. Kobayashi et al., J. Appl. Phys. 12 (1973) 1637.
[9] X.M. Xu et al., J. Lumin. 36 (1986) 101.
[10] C.C. Yu et al., Luminescence and Display 5 (1984) 12 (in Chinese).
[11] L.J. Meng, Thesis, Changchun, Inst. of Physics (1986).
[12] J.F. Porter et al., Phys. Rev. 152 (1966) 300.
[13] R. Reisfeld, Structure and Bonding 13 (1973) 53.